Journal of Alloys and Compounds 509 (2011) 1626–1629

Contents lists available at ScienceDirect

Journal of Alloys and Compounds

journal homepage: www.elsevier.com/locate/jallcom

Nanocrystallization-induced large room-temperature compressive plastic strain of $Ti_{40}Zr_{25}Ni_8Cu_9Be_{18}$ BMG

J.N. Mei[a,b,c], J.L. Soubeyroux[b,*], J.J. Blandin[c], J.S. Li[a], H.C. Kou[a], H.Z. Fu[a], L. Zhou[a]

[a] State Key Laboratory of Solidification Processing, Northwestern Polytechnical University, Xi'an 710072, Shaanxi, PR China
[b] Institut Néel/CRETA, CNRS Grenoble, 25 Avenue des Martyrs, BP 166, 38042 Grenoble Cedex 9, France
[c] Grenoble-INP, SIMAP-GPM2, CNRS, 38402 Saint-Martin d'Hères Cedex, France

ARTICLE INFO

Article history:
Received 19 May 2010
Received in revised form
10 November 2010
Accepted 11 November 2010
Available online 21 November 2010

Keywords:
Bulk metallic glass
Titanium alloy
Microstructure
Quenched-in nuclei
Nanocrystallization
Plastic strain

ABSTRACT

By combining neutron diffraction, high-resolution transmission electron microscopy and thermal analysis measurements, the microstructure of as-cast $Ti_{40}Zr_{25}Ni_8Cu_9Be_{18}$ BMG with diameter of 2 mm was identified to be quenched-in nuclei/amorphous matrix. The quenched-in nuclei transform to $(Ti,Zr)Be_2$ nanocrystals with the average size of 4 nm homogeneously distributed into the amorphous matrix during deformation, which could be responsible for the large room-temperature compressive plastic strain, up to 8.0% at a constant strain rate of $5 \times 10^{-4}\ s^{-1}$.

1. Introduction

Ti-based bulk metallic glasses (BMGs) have attracted widespread attention for their scientific importance and potential applications as lightweight structural materials [1–10]. Ti-rich Ti–Zr–Ni–Cu–Be alloys are typical Ti-based BMGs, generally have good combination of GFA and mechanical properties, especially large room-temperature compressive plastic strain [5–10]; however, the reason why Ti–Zr–Ni–Cu–Be BMGs exhibit large compressive plastic strain is not clear, and still in argument. Park et al. [8] found that the Ti-rich Ti–Zr–Ni–Cu–Be BMGs whose first crystallization product was quasicrystalline phase generally exhibited relatively large plastic strain, and attributed the enhancement of plastic strain to the existence of quenched-in icosahedral nuclei embedded in the amorphous matrix. While recently, Fornell et al. [10] argued that the intrinsic plasticity of Ti–Zr–Ni–Cu–Be BMGs was due to its elastic properties, namely, the relatively good plasticity was related to rather low ratio of elastic shear modulus (μ) to bulk modulus (B), μ/B. In addition, Ohkubo et al. [9] argued that the plasticity of $Ti_{40}Zr_{25}Cu_{12}Ni_3Be_{20}$ alloy does not originate from the glassy phase itself but is closely related to the amount of nanocrystals embedded in the metallic glass matrix.

The mechanical response for a material is correlated with its microstructure. In addition, for metallic glasses, since their characteristic of thermodynamic metastability, the structural changes during deformation caused by strain energy should also be considered during the analysis of deformation behavior. So, it is possible to construct the correlation between the large room-temperature plastic strain and the structural instability of metallic glasses.

In this study, we present the large room-temperature compressive plastic strain (up to 8.0% at a strain rate of $5 \times 10^{-4}\ s^{-1}$) of $Ti_{40}Zr_{25}Ni_8Cu_9Be_{18}$ BMG, and a discussion based on the analysis of structural nature of the as-cast sample and its structural changes during deformation. The nanocrystallization of the quenched-in nuclei in the amorphous matrix during deformation should be responsible for the enhancement of plastic strain.

2. Experiment

The ingots of master alloy with nominal composition of $Ti_{40}Zr_{25}Ni_8Cu_9Be_{18}$ (at.%) were prepared by melting elements of 99.8–99.999 wt.% purity with high frequency electromagnetic induction in a water-cooled copper crucible under a high purity argon atmosphere. The ingot alloys were remelted at high temperature several times to ensure the compositional homogeneity. Cylindrical specimens with 2 mm in diameter and 40 mm in length were prepared by injection casting into a water-cooled copper mould via an electromagnetic levitation-melt state under a high purity argon atmosphere before casting to obtain a completely melted state. Alloy's oxygen content was measured <400 ppm. DSC parameters measured at

* Corresponding author. Tel.: +33 0476889039; fax: +33 0476881280.
E-mail address: jean-louis.soubeyroux@grenoble.cnrs.fr (J.L. Soubeyroux).

0925-8388/$ – see front matter © 2010 Elsevier B.V. All rights reserved.
doi:10.1016/j.jallcom.2010.11.071

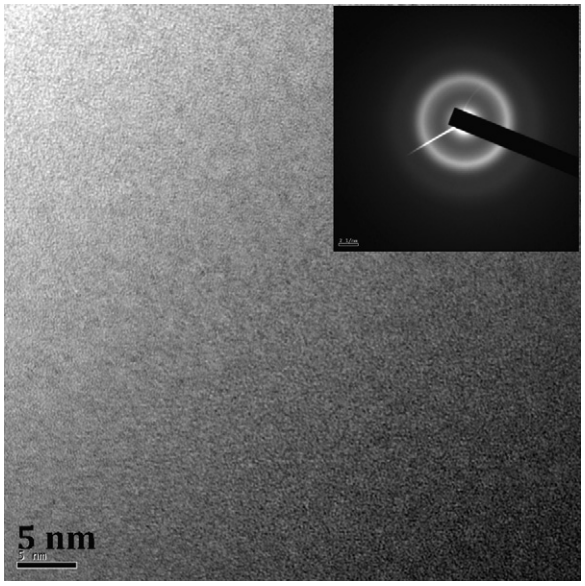

Fig. 1. TEM and corresponding SADP of $Ti_{40}Zr_{25}Ni_8Cu_9Be_{18}$ BMG.

10 K/min are: $\Delta T = 53$ K between $T_g = 575$ K and first crystallization peak $T_{x1} = 628$ K [11].

The glassy state of alloy was examined by high-resolution transmission electron microscopy (HRTEM, JEM-3010). Isothermal crystallization was studied using differential scanning calorimetry (DSC, Netzsch DSC 404 s) in a flowing argon atmosphere.

Uniaxial compression tests were performed on cylindrical rods of 2 mm in diameter and 3.5 mm in length by using a MTS 4 M testing machine at room-temperature with constant strain rate of $5 \times 10^{-4}\ s^{-1}$. The sample end surfaces were polished to be parallel to each other and perpendicular to the loading axis. BN powder was used as lubricant to reduce friction between testing samples and the platen of the machine. The fractured samples were observed in a JEOL-JSM6400 scanning electron microscope (SEM) and TEM.

3. Results

3.1. Microstructure identification of as-cast $Ti_{40}Zr_{25}Ni_8Cu_9Be_{18}$ BMG

Fig. 1 shows a bright-field TEM image with inset of selected-area electron diffraction pattern (SADP) from the as-cast $Ti_{40}Zr_{25}Ni_8Cu_9Be_{18}$ alloy, reveals a uniform, featureless homogeneous contrast, lacking any long-range topological order, no regularity of the lattice fringes and a series of diffuse halo rings, respectively, indicating a monolithic amorphous phase.

Here, we recall the results obtained in the in-situ neutron diffraction investigation performed on the as-cast $Ti_{40}Zr_{25}Ni_8Cu_9Be_{18}$ alloy which has been presented in Ref. [11] using $\lambda = 2.534$ Å. At the beginning of the experiment, the characteristic diffraction pattern of an amorphous compound with short range order (bump maximum at $2\theta = 68^\circ$ $d = 2.257$ Å) is observed. At 610 K (608 K in DSC experiment), some new peaks appear at $2\theta = 39.34^\circ$ and 65.54° corresponding to d spacings 3.749 and 2.332 Å, respectively, these peaks are diffuse at the beginning and correspond certainly to very tiny crystals, then sharper with time and temperature increasing. With only 2 peaks it is difficult to ascertain a phase, but we can exclude some hypothesis, in particular α- or β-Ti, which did not present a peak at $d = 3.749$ Å. In the same way the icosahedral phase often observed in phases with beryllium presents a double peak around $d = 2.34$ Å. In simple binary phases, only the $TiBe_2$ (fcc, $a = 6.45$ Å) phase presents 2 peaks close to the observed peaks, by refining the cell parameter, the value $a = 6.603$ Å has been determined. It could be explained by a partial replacement of Ti by a bigger atom such as zirconium. However the $ZrBe_2$ compound is hexagonal, so only partial replacement must be assumed.

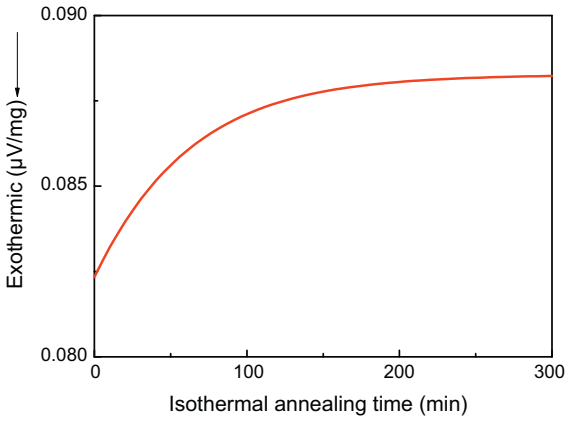

Fig. 2. Isothermal annealing DSC curve obtained from as-cast $Ti_{40}Zr_{25}Ni_8Cu_9Be_{18}$ alloy.

The formation of the (Ti,Zr)Be_2 phase as primary crystallization phase (PCP) is in agreement with previous primary crystallization studies of BMG containing beryllium phase. We have observed, during the crystallization of $Zr_{46.75}Ti_{8.25}Cu_{7.5}Ni_{10}Be_{27.5}$ phase, the formation of $ZrBe_2$ and a quasicrystalline phase [12] as PCP and whose TEM images are very similar in shape and size. Depending on the history of the glass formation (sample diameter, cooling technique, oxygen presence), different phases can be formed because of the different atomic structures (short range order) possible in the glass state. It is why the observations of Kim et al. [7] of a quasicrystalline phase as PCP may be also the result of the BMG synthesis process, different from our samples. More information about the in-situ neutron diffraction study of $Ti_{40}Zr_{25}Ni_8Cu_9Be_{18}$ alloy upon heating has been presented in Ref. [11].

However, the isothermal DSC curve (at 340 °C, in the glass transition region, see Fig. 2) shows a monotonically decreasing calorimetric signal, which is the evidence that the crystallization process involves only the grain coarsening or growth of quenched-in nuclei. For grain coarsening or growth of quenched-in nuclei, the kinetics of the two processes is fundamentally different although they may exhibit similar calorimetric behavior. Growth of quenched-in nuclei in metallic glasses involves a solid state transformation from an amorphous state to a crystalline state, while grain coarsening occurs in micro-crystalline or nanocrystalline materials just corresponding to the reduction in interface enthalpy due to the annihilation of grain boundaries. Obviously, for $Ti_{40}Zr_{25}Ni_8Cu_9Be_{18}$ BMG, no crystals can be detected by neutron diffraction and HRTEM measurements, confirming the growth of quenched-in nuclei as the origins for the decreasing calorimetric signal. Actually, we have performed non-isothermal DSC to investigate the crystallization mechanism (see Ref. [13]), and the calculated Avrami exponent n for the first crystallization event falls in the range of 1.4–1.6, implying a diffusion-controlled three-dimensional growth of pre-existing nuclei for the first crystallization event, as also confirms the quenched-in nuclei/amorphous matrix structure of the as-cast $Ti_{40}Zr_{25}Ni_8Cu_9Be_{18}$ BMG.

3.2. Room-temperature compressive properties of as-cast $Ti_{40}Zr_{25}Ni_8Cu_9Be_{18}$ BMG

Fig. 3 shows a typical room-temperature uniaxial compressive true strain–stress (σ–ε) curve of as-cast $Ti_{40}Zr_{25}Ni_8Cu_9Be_{18}$ BMG deformed at a constant strain rate of $5 \times 10^{-4}\ s^{-1}$. It is found that it shows a large elastic strain of 2.1%, and had a maximum strength of

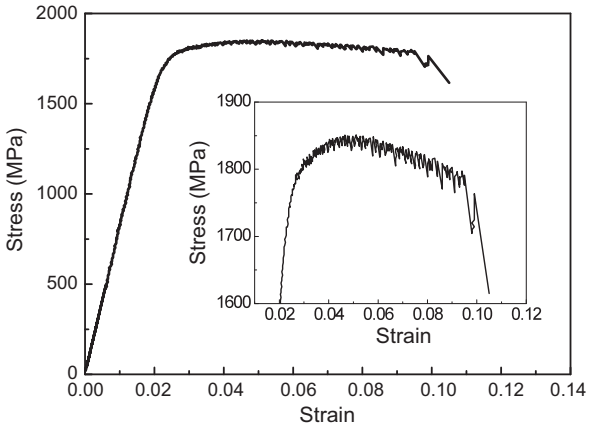

Fig. 3. Room-temperature compressive stress–strain (σ–ε) curve at a constant strain rate of $5 \times 10^{-4}\ s^{-1}$ for as-cast $Ti_{40}Zr_{25}Ni_8Cu_9Be_{18}$ BMG. The inset shows the enlarged image of the serrated flow.

1850 MPa and a considerable plastic strain of 8.0%. In addition, after yielding, obvious serrated flow can be observed (see the enlarged image in Fig. 3). The occurrence of inhomogeneous plastic flow indicates the initiation and propagation of individual shear bands during quasistatic loading [14]. And in these shear bands there is a sudden decrease of viscosity [15], which brings about load drops and a concomitant mechanical softening.

Fig. 4 shows the outer surfaces of the fractured $Ti_{40}Zr_{25}Ni_8Cu_9Be_{18}$ sample. Surprisingly, the multiple shear bands including primary shear bands and branched secondary shear bands (see Fig. 4(b)) are distributed homogeneously over the whole surface, explaining the large plastic strain observed during compressive deformation.

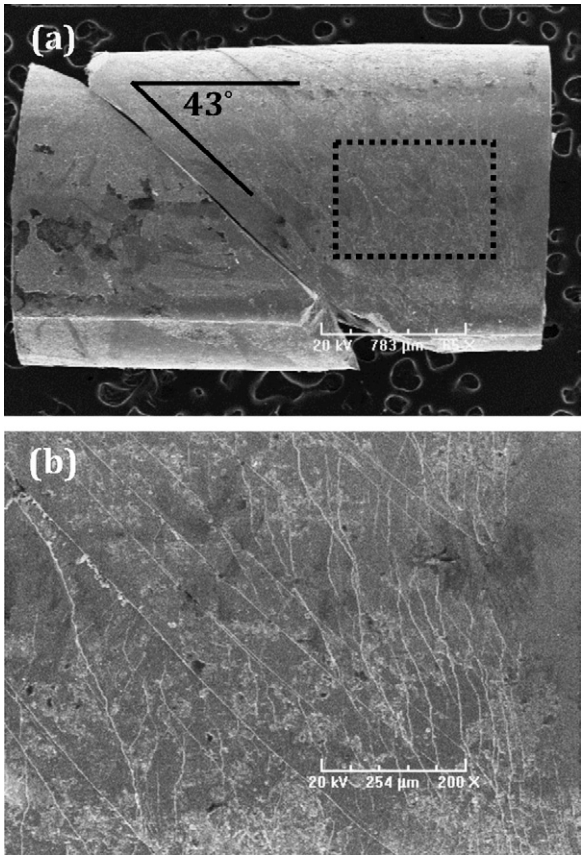

Fig. 4. (a) View of outer surface of the $Ti_{40}Zr_{25}Ni_8Cu_9Be_{18}$ sample deformed at the strain rate of $5 \times 10^{-4}\ s^{-1}$ and (b) higher magnification of shear bands in the black rectangle area.

It is well known that for common BMGs, one major shear band dominates the deformation and results in a sudden fracture, in this study we found multiple shear bands on the outer surface of fractured $Ti_{40}Zr_{25}Ni_8Cu_9Be_{18}$ BMG, suggesting that a large number of shear bands simultaneously operate during the plastic deformation, the reason will be discussed in the following section.

4. Discussion

The dissimilar intrinsic plasticity or brittleness in different BMG systems is essentially due to their different nature, e.g. (i) properties of constituent elements and composition, (ii) and structural configurations. It was reported that the high metalloid content as well as the presence in major quantities of a metallic constituent that has a body centered cubic structure in its crystalline state (e.g. Mg-based metallic glasses), leads to intrinsic brittleness [16]. Spaepen [15] proposed that shear bands are initiated as a result of coalescence of the free volume, which was later confirmed by HRTEM [17]. Sung et al. [18] argued that alloys with a low melting temperature usually exhibit large plastic strain. In addition, the elastic moduli are apparently important parameters as a chain to understand the correlation between the structural characteristics and relevant mechanical properties. Lewandowski et al. [19] pointed out that the intrinsic plasticity or brittleness of metallic glasses is correlated with their Poisson's ratio, ν. The larger the ν is, the more ductile the metallic glasses become. Metallic glasses with a high Poisson's ratio $\nu > 0.31$–0.32 or, equivalently, a ratio of elastic shear modulus (μ) to bulk modulus (B), μ/B, less than 0.41–0.43, are ductile. The value of μ/B for $Ti_{40}Zr_{25}Ni_8Cu_9Be_{18}$ metallic glass is measured to be 0.314, which is higher than that for Pd-based and Pt-based metallic glasses ($\mu/B > 0.18$) however lower than that for some more brittle metallic glasses ($\mu/B > 0.43$ for Mg-based and Ce-based metallic glasses) and oxide glasses ($\mu/B > 0.7$) [10], indicating its moderate plasticity.

Park et al. [8] found that the Ti-rich Ti–Zr–Ni–Cu–Be BMGs whose first crystallization product was quasicrystalline phase generally exhibited relatively large plastic strain, and attributed the enhancement of plastic strain to the existence of quenched-in icosahedral nuclei embedded in the amorphous matrix. However, for $Ti_{40}Zr_{25}Ni_8Cu_9Be_{18}$ BMG, the first crystallization product is not a quasicrystalline phase but (Ti,Zr)Be_2 phase, implying that the large plastic strain should be independent on the properties of primary phase, there must be other reason being responsible for the large compressive plastic strain of $Ti_{40}Zr_{25}Ni_8Cu_9Be_{18}$ BMG.

The TEM image for the fractured $Ti_{40}Zr_{25}Ni_8Cu_9Be_{18}$ BMG under the condition of room-temperature compression at a constant strain rate of $5 \times 10^{-4}\ s^{-1}$ is shown in Fig. 5. It can be seen that nanocrystals with an average size of 4 nm are homogeneously embedded in the amorphous matrix, demonstrating the occurrence of the transformation from quenched-in nuclei to nanocrystals during deformation. The formation of the nanocrystals may be due to the supply of the mechanical energy during compression, which is associated with its low thermal stability (activation energy for its first crystallization event is 235.2 kJ/mol [13]) [20], implying that the large plastic strain may be dependent on the thermal instability upon heating.

It is well known that the nanocrystals may significantly affect the mechanical behavior of metallic glasses through the interaction with shear bands. Such nanocrystals become inhomogeneous energy barriers, and a propagating shear band might be forced to be deflected or branched when it reaches the high energy barrier region. This would result in the initiation of new shear bands.

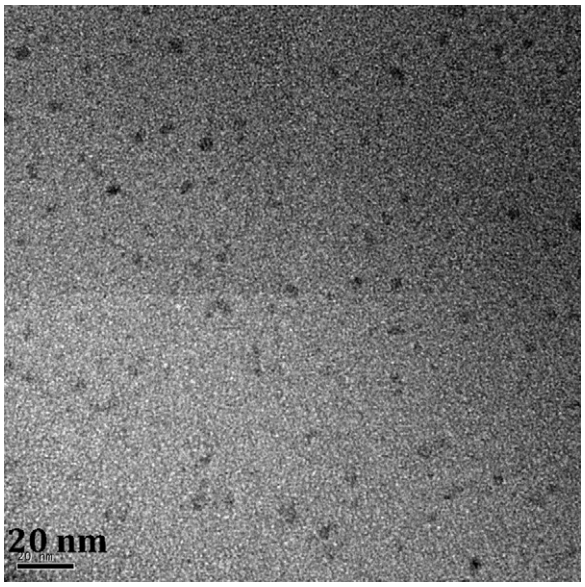

Fig. 5. TEM image of the fractured $Ti_{40}Zr_{25}Ni_8Cu_9Be_{18}$ BMG.

The increase of the total area of shear bands due to the formation of multiple shear bands and deflection in the individual shear bands lead to appreciable macroscopic plasticity at low strain rate. For example, it was reported recently that the as-cast $Cu_{50}Zr_{50}$ BMGs exhibited a compressive plastic strain of more than 50% at room-temperature due to a dispersion of embedded nanocrystals, which was explained by the suppression of shear softening through nanocrystal coalescence [21].

Based on the analysis above, the large compressive plastic strain of $Ti_{40}Zr_{25}Ni_8Cu_9Be_{18}$ BMG may result from its high value of Poisson's ratio (or low value of the ratio of elastic shear modulus (μ) to bulk modulus (B)) as well as the homogeneous nanocrystallization of the quenched-in nuclei during deformation due to its low thermal stability which can disperse the strain localization upon compressive loading, resulting in the generation of multiple shear bands.

5. Conclusions

The microstructure of as-cast $Ti_{40}Zr_{25}Ni_8Cu_9Be_{18}$ BMG was identified for the first time by combining neutron diffraction, high-resolution transmission electron microscopy and thermal analysis measurements, and the room-temperature compression test was also performed on this alloy. It is found the existence of quenched-in nuclei in the amorphous matrix for the as-cast sample. The primary crystallization phase is not I-phase as previously reported, but (Ti,Zr)Be_2 phase, which may result from the different history of the glass formation. The large room-temperature compressive plastic strain up to 8.0% at a constant strain rate of $5 \times 10^{-4}\ s^{-1}$ could be mainly attributed to the nanocrystallization of the quenched-in nuclei during deformation which is correlated with the thermal instability of the quenched-in nuclei in addition to its high value of Poisson's ratio (or low value of the ratio of elastic shear modulus (μ) to bulk modulus (B)).

Acknowledgements

This work was supported by National Natural Science Foundation of China (50601011), National Basic Research Program of China (2007CB607603), Fundamental Research Project of National Defense of China (A2720060295) and China Scholarship Council. We are very grateful to Q. Wang for helpful advice.

References

[1] G. Duan, A. Wiest, M.L. Lind, A. Kahl, W.L. Johnson, Scr. Mater. 58 (2008) 465–468.
[2] C.L. Ma, S. Ishihara, H. Soejima, N. Nishiyama, A. Inoue, Trans. JIM 45 (2004) 1802–1806.
[3] C.L. Ma, H. Soejima, S. Ishihara, K. Amiya, N. Nishiyama, A. Inoue, Mater. Trans. JIM 45 (2004) 3223–3227.
[4] K.B. Kim, X.F. Zhang, S. Yi, M.H. Lee, J. Das, J. Eckert, Philos. Mag. Lett. 88 (2008) 75–81.
[5] F.Q. Guo, H.J. Wang, S.J. Poon, G.J. Shiflet, Appl. Phys. Lett. 86 (2005) 091907.
[6] Y.C. Kim, J.H. Na, J.M. Park, D.H. Kim, Y.H. Lee, W.T. Kim, Appl. Phys. Lett. 83 (2003) 3093–3095.
[7] Y.C. Kim, W.T. Kim, D.H. Kim, Mater. Sci. Eng. A 375–377 (2004) 127–135.
[8] J.M. Park, H.J. Chang, K.H. Han, W.T. Kim, D.H. Kim, Scr. Mater. 53 (2005) 1–6.
[9] T. Ohkubo, D. Nagahama, T. Mukai, K. Hono, J. Mater. Res. 22 (2007) 1406–1413.
[10] J. Fornell, A. Concustell, S. Suriñach, W.H. Li, N. Cuadrado, Int. J. Plast. 25 (2009) 1540–1559.
[11] J.L. Soubeyroux, J.N. Mei, J. Alloys Compd. 504S (2010) S239–S242.
[12] B. Van De Moortèle, T. Epicier, J.L. Soubeyroux, J.M. Pelletier, Philos. Mag. Lett. 84 (2004) 245–256.
[13] J.N. Mei, thesis, Joseph Fourier University & Northwestern Polytechnical University, 2009.
[14] C.A. Schuh, T.C. Hufnagel, U. Ramamurty, Acta Mater. 55 (2007) 4067–4109.
[15] F. Spaepen, Acta Mater. 23 (1977) 407–415.
[16] U. Ramamurty, M.L. Lee, J. Basu, Y. Li, Scr. Mater. 47 (2002) 107–111.
[17] J. Li, Z.L. Wang, T.C. Hufnagel, Phys. Rev. B 65 (2002) 144201.
[18] D.S. Sung, O.J. Kwon, E. Fleury, K.B. Kim, J.C. Lee, D.H. Kim, Y.C. Kim, Met. Mater. Int. 10 (2004) 575–579.
[19] J.J. Lewandowski, W.H. Wang, A.L. Greer, Philos. Mag. Lett. 85 (2005) 77–87.
[20] S.W. Lee, M.Y. Huh, E. Fleury, J.C. Lee, Acta Mater. 54 (2006) 349–355.
[21] A. Inoue, W. Zhang, T. Tsurui, A.R. Yavari, A.L. Greer, Philos. Mag. Lett. 85 (2005) 221–237.